Mottram, N. J., & Hogan, S. J. (1997). Multiple solutions in twisted nematic liquid crystal layers.

Multiple Solutions in Twisted Nematic Liquid Crystal Layers

by N. J. Mottram* and S. J. Hogan
Department of Engineering Mathematics, University of Bristol,
Queens Building, University Walk, Bristol, BS8 1TR, England

Abstract

A twisted nematic layer is modelled using a continuum theory which allows for the presence of phase changes and biaxiality within liquid crystals. Under certain approximations analytical solutions are found and used to validate numerical solutions of the full problem. Using a numerical continuation package (AUTO) it is possible to find regions where multiple solutions for the director configuration and hysterisis can occur. Changes in temperature, amount of twist and gap width are investigated in detail and subsequently the relevance of these results to display technology is discussed.

* Author for correspondence
Running title: Theory of Twisted NLCs

1 Introduction

The widespread use of liquid crystal technology has led to significant interest and research into all aspects of liquid crystals . Theoretical research into this field only gained momentum, more than a hundred years after the first liquid crystal was discovered, with the formulation of a continuum model by Frank [10] and Oseen [15] which could predict the static behaviour of nematic liquid crystals. Since then with the emergence of many different types of liquid crystal such as chiral nematic, smectic and columnar, the volume of research has increased dramatically. Nevertheless even the simplified equations governing the static problem of a nematic display configuration are not fully understood.

The nematic liquid crystalline state which exists in certain materials is a mesomorphic state that occurs in a temperature range between the liquid and the solid (crystalline) phases. In this intermediate state the molecules tend to align along a preferred direction. It is the presence of this orientational order in the material which leads to an optical and electromagnetic anisotropy which may be exploited in the production of displays. The orientational order inherent in the liquid crystalline state is described in terms of *directors* (Figure 1), representing the locally averaged direction of the molecules at a point in the material, and certain variables measuring how aligned the molecules are with these average direction vectors. A continuum theory for liquid crystals can then be derived using these macroscopic quantities.

The continuum theory of Frank [10] and Oseen [15] describes the static behaviour of nematic liquid crystals. While this theory has been successfully used to investigate many types of defects it depends on the assumption that the liquid crystal is uniaxial (i.e. there is only one director $\mathbf{n}$ so the ellipses of Figure 1 are replaced by circular rods) and that if the order changes within the nematic sample it changes between liquid crystalline and isotropic. It does not allow a rigorous mathematical description of areas of high deformation such as the region near to a defect where the energy is predicted to be infinite in value.

The need to fully describe these regions in a continuum model has led to the formulation by Ericksen of a new equilibrium theory [8]. He considers a

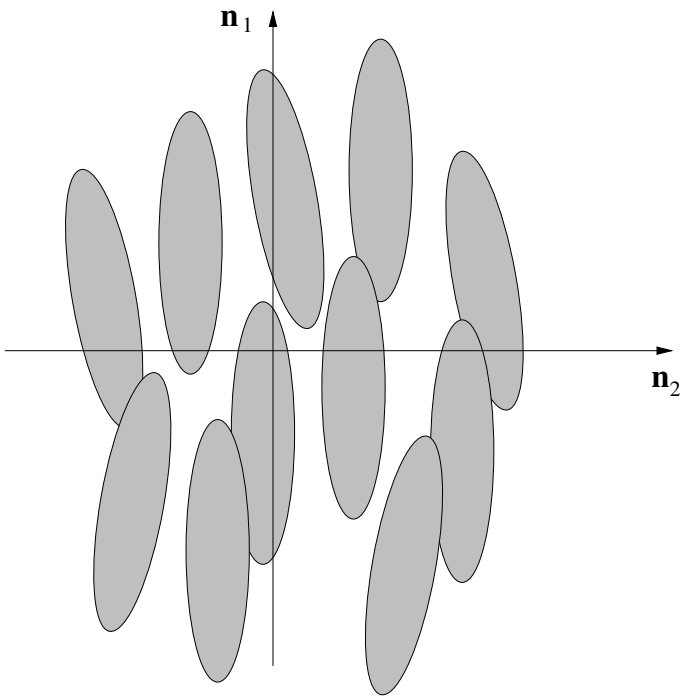

Figure 1: Simplistic representation of biaxial nematic liquid crystal with directors $\mathbf{n}_1$ and $\mathbf{n}_2$ defined as the average directions of the major and minor axis of *flat*, elliptical molecules [5].

uniaxial nematic (the single director $\mathbf{n}$ is defined as the average direction of the *major* molecular axis) where the degree of order of the liquid crystal can be represented by a *scalar order parameter* S, defined as a local orientational order of the molecules,

$$S = \frac{1}{2} < (3\cos^2\psi - 1) > \tag{1.1}$$

where ψ is the angle between a molecule and the director and $<>$ denotes a thermal average (see for example de Gennes and Prost Section 2.1.1 [5]). Therefore when $S = 0$ the molecules are oriented in a random fashion and the material is isotropic and when $S = 1$ the molecules are perfectly ordered with the director and the material is crystalline. When $S = -1/2$ the molecules are all perpendicular to the director. In this paper we will only consider $0 \leq S \leq 1$. In Ericksen [8] S is allowed to vary spatially in the governing equations so that there may be regions of *different* order within the sample. The free energy, which is now a function of $\mathbf{n}$ and S, includes the free energy from the Frank-

Oseen theory *multiplied by a function of* S which vanishes at a defect, removing the singularity in the free energy. This new theory can therefore describe changes to the order S in a rigorous mathematical framework.

This approach had been anticipated by earlier authors such as de Gennes [4] and Fan [9]. Other authors have used Landau-de Gennes theory to investigate the core structure of disclination lines [11, 17, 13] and more recently Virga and Biscari [16, 18, 2] have used these theories to study biaxial nematic liquid crystals in various geometries.

We will use such a continuum theory to investigate the most common liquid crystal display in use today, the twisted nematic liquid crystal display (TNLCD).

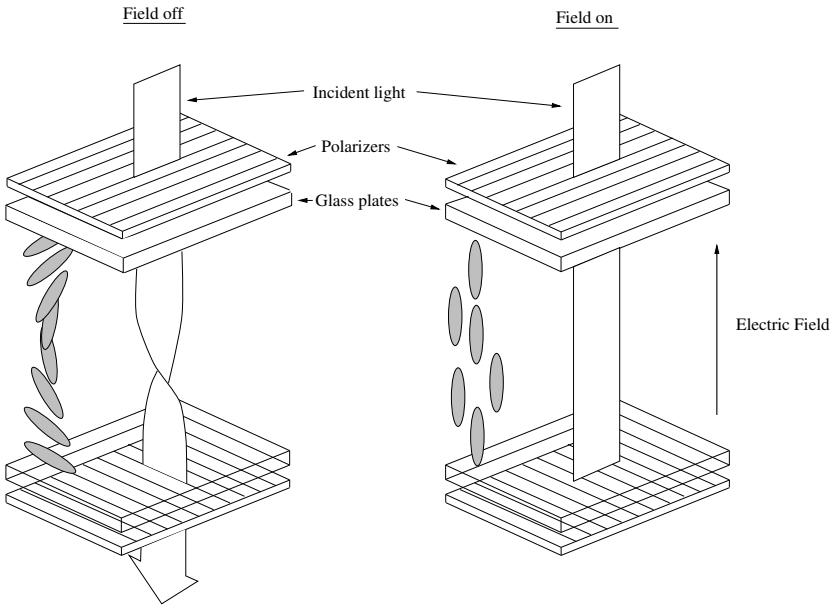

Figure 2: The Twisted Nematic Liquid Crystal Display.

The TNLCD (Figure 2) is constructed so that without an applied electric field, the liquid crystal molecules are forced (by treated glass plates) to form a helical structure. The nature of this molecular configuration is such that light passing through the upper polariser is guided to align with and hence pass through the bottom polariser. When an electric field (greater than some critical value E_c) is applied to the layer, the molecules are forced to rotate to align with the field. The twisted structure is therefore destroyed and hence

can not guide the light through the bottom polariser. The display transmits light when no field is applied and blocks light when a field is applied. The advantages of using such a display are that the threshold voltage is low, around a few volts, and that there is a high contrast between the on (black) and off (white) states. The disadvantages are that the display will only work well when viewed straight on, the switching times between states are slow, the use of two polarizers means that transmission is low and the display may appear patchy since some regions twist clockwise and some twist anti-clockwise. However it has been found that if the nematic is chiral (it has a *natural* twist in one direction) a better performance is acheived.

Although it is thought that in normal situations a TNLCD can be described satisfactorly with Frank-Oseen theory there will be occasions when twist *will* cause changes in the orientational order S. One such occasion occurs when the temperature of the TNLCD is close to the critical temperature where the undistorted nematic liquid crystal undergoes a phase change to an isotropic liquid. As will be seen later the region around the twist distortion has low orientational order and the presence of this region can affect the phase change in a similar way to recent work by the authors [13] where a disclination line was seen to affect the critical temperature.

Another occasion is when the TNLCD contains regions of different amounts of twist so that *reverse twist* and *cholesteric unwinding* may occur. If the director is zero on the lower boundary and ϕ_d on the upper boundary, then the director may twist from zero to $\phi_d + n\pi$, for any positive or negative integer n, within the cell and still satisfy the boundary conditions. Reverse twist occurs when $n = -1$ and cholesteric unwinding describes the transition from the state $n = i$ to $n = i-1$. Frank-Oseen theory cannot model transitions between these topologically different states but by introducing the possiblility of a reduction in the orientational order it is possible to change from one twist state to another. In this paper we attempt to model the necessary reduction in orientational order and leave the transition process for future work.

There are other occasions where twist induced changes in the scalar order parameters may be important such as the recently demonstrated In-Plane switching device [14] or the Bistable Twisted Nematic device [1]. For their future success as display devices it is necessary to understandig the importance

of changes of orientational order within the cell.

In all of these examples it is twist deformation that would induce any change in the orientational order S. We will therefore use a continuum theory which is able to describe such changes to consider the *field off* state of a nematic in a TNLCD which contains all the essential features of these examples.

We obtain analytical solutions under certain restricting approximations and then using the numerical continuation package AUTO [6] the full equations are solved. It is then possible to follow the solution as the system parameters are altered and it is found that for certain parameter regions mutiple director configurations exist.

In Section 2 we introduce the governing equations used by Virga [18] in detail and subsequently the equations and boundary conditions for a twist layer are presented. In Sections 3 and 4 certain analytical solutions are found and in Section 5 a numerical investigation of the full equations is presented and it is found that in some parameter regions there exist multiple solutions. It is possible to switch from one solution to another by altering certain critical parameters and this process forms a hysterisis loop. In Section 6 these results are discussed.

2 Governing Equations

In attempting to describe the behaviour of a liquid crystal material we use a continuum theory based on a Landau-de Gennes expansion of the free energy [4] or similarly the approach used by Ericksen [8]. These methods take the free energy of the system $\mathcal{F}$ to be the sum of the energy due to the spatial distortions of the liquid crystal and the energy due to the deviation from some minimum energy state. In this paper we follow Biscari and Virga [2] where the free energy is a function of the major axis director orientation angle ϕ (Fig. 3) the phase variable S and the degree of biaxiality α. The variables S and α represent the local orientational order of the liquid crystal about the director $\mathbf{n} = (\sin\phi,\ \cos\phi,\ 0)$ and the direction perpendicular to $\mathbf{n}$ and the z-axis. We have therefore used the assumption that both $\mathbf{n}_1$ and $\mathbf{n}_2$ from Figure 1 are in the xy-plane.

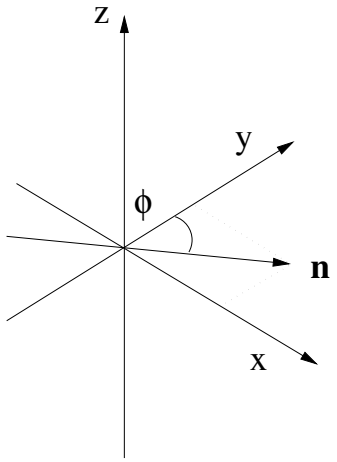

Figure 3: The director $\mathbf{n}$ (in the xy-plane) and the director angle ϕ

The equations governing the behaviour of the liquid crystal are then the Euler-Lagrange equations obtained by minimising the free energy $\mathcal{F}$ for variations in ϕ, S and α. These equations may be solved subject to certain appropriate boundary conditions in order to model a twist layer.

The free energy is the sum of distortional and potential energies,

$$\mathcal{F} = \int_V F_D \mathrm{dv} = \int_V \frac{K}{2}\,(F_{dist} + F_{pot})\mathrm{dv} \tag{2.2}$$

where F_D is the free energy density and the potential energy F_{pot} is assumed

to be the sum of two functions of S and α modelling the effects on the free energy of changes in phase and biaxiality respectively,

$$F_{pot} = \sigma(\mathbf{Q}) = \kappa_1\sigma_1(S) + \kappa_2\sigma_2(\alpha) \tag{2.3}$$

where κ_1 and κ_2 are positive material constants. The first potential has been studied by both de Gennes [4] and Doi [7] and can be written as,

$$\sigma_1(S) = AS^4 + BS^3 + CS^2 + D \tag{2.4}$$

where the coefficients A, B, C, and D are temperature dependent material parameters. The quantity D contributes a constant term to the free energy and can be neglected since it does not affect the minimisation of the free energy. The suitably scaled potential may therefore be rewritten as,

$$\sigma_1(S) = S^2\left(\frac{S^2}{4} - (S_u + S_b)\frac{S}{3} + \frac{S_uS_b}{2}\right) \tag{2.5}$$

so that when there are two non-zero turning points they occur at $S = S_u > 0$ and $S = S_b > 0$. This quartic potential models the ability of the material to have a local minimum energy at two values of S, the first at $S = 0$ when the material is isotropic and the second at $S = S_b$ when the material is liquid crystalline. The effect of temperature changes on this potential can now be described in terms of the parameters S_u and S_b or, if we use the nondimensionalised variable $S^* = S/S_b$, the parameter S_u^*. Then the turning points occur at $S = 0$, S_u^* and 1. If we fix S_b the effect on the potential function $\sigma_1(S)$ is shown in Figure 4 where it is assumed that $S_b = 0.7$ as will be used throughout this paper.

The second potential σ_2 represents the capacity for the material to support biaxial states. If it is assumed that the nematic is uniaxial in the temperature range $S_u^* \in (0, 1)$ then σ_2 will have a minimum at $\alpha = 0$. This form of the σ_2 potential does not *disallow* biaxial states but any variance from a uniaxial state will result in an increased free energy. It is therefore expected that regions of biaxiality will only occur when their presence will reduce the distortional energy term in equation (2.2) such as at the core of the disclination where there is a high amount of distortion. Following Virga [2], the simplest form of such a potential,

$$\sigma_2(\alpha) = \frac{\alpha^2}{2} \tag{2.6}$$

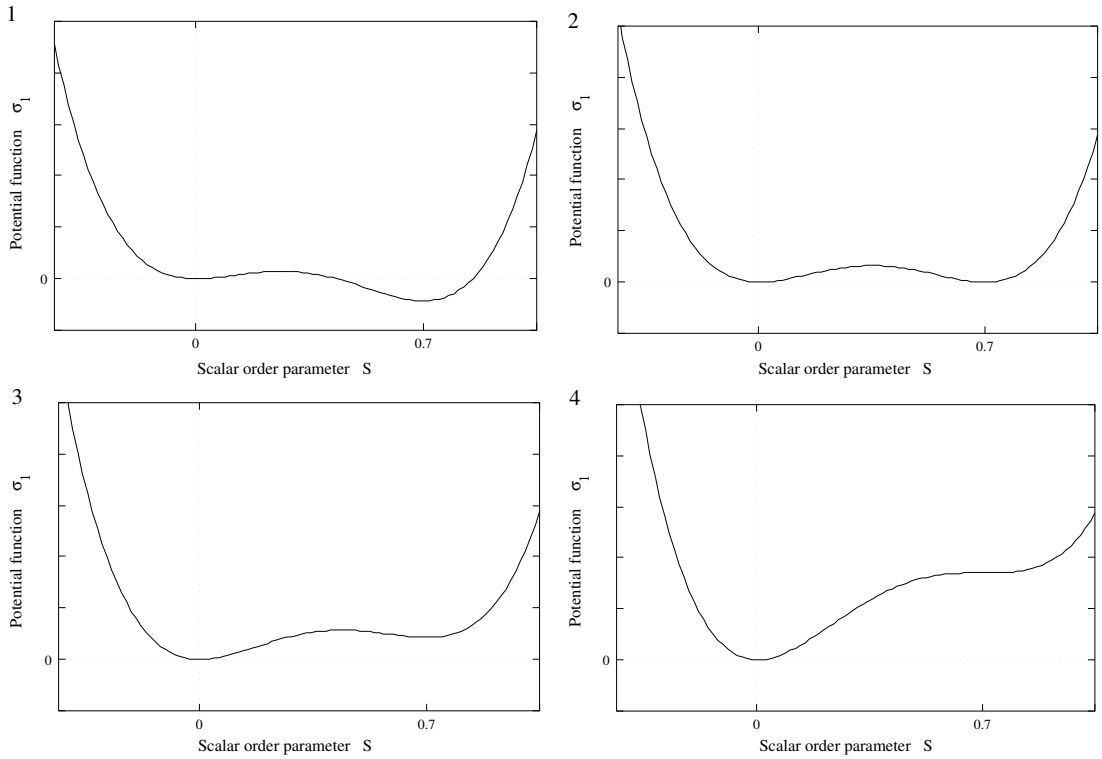

Figure 4: Scalar order parameter energy potential $\sigma_1(S)$ for $S_b = 0.7$ at temperatures 1. $T \in (T^*, T_c)$ or equivalently $S_u \in (0,\ S_b/2)$ or $S_u^* \in (0,\ 1/2)$, 2. $T = T_c$, $S_u = S_b/2,\ S_u^* = 1/2$, 3. $T \in (T_c, T_+)$, $S_u \in (S_b/2,\ S_b)$ or $S_u^* \in (1/2,\ 1)$, 4. $T = T^+,\ S_u = S_b,\ S_u^* = 1$

is used.

With the above potentials (2.5, 2.6) the free energy density becomes,

$$\begin{aligned} F_D &= \frac{K}{2}\left(2(S-\alpha)^2(\nabla\phi)^2 + \frac{2}{3}(\nabla S)^2 + 2(\nabla\alpha)^2 \right. \\ &\quad \left. + \kappa_1 S^2\left(\frac{S^2}{4} - (S_u+S_b)\frac{S}{3} + \frac{S_u S_b}{2}\right) + \frac{\kappa_2}{2}\alpha^2\right) \end{aligned} \tag{2.7}$$

The first term in this equation is simply the Frank free energy density multiplied by a function of S and α. As discussed in the introduction, this function will vanish when the Frank energy contains a singularity in order to ensure the free energy of the system remains finite. The second and third terms in (2.7) are the energy densities associated with changes in the scalar order parameters S and α and the last two terms are the internal potentials mentioned above. Although the director distortions do not lead to a singularity in the Frank free energy in the situation considered in this paper, the concentration of this distortional free energy density into a small region of the cell will cause a significant reduction in the function $(S-\alpha)^2$ in order to minimise the free energy of the system.

The Euler-Lagrange equations with respect to the dependent variables ϕ, α and S are,

$$0 = \nabla^2 S - 3(S-\alpha)\left(\nabla\phi\right)^2 - \frac{3\kappa_1}{4}S(S-S_u)(S-S_b) \tag{2.8}$$

$$0 = \nabla^2\alpha + \left(S-\alpha\right)\left(\nabla\phi\right)^2 - \frac{\kappa_2}{4}\alpha \tag{2.9}$$

$$0 = (S-\alpha)\nabla^2\phi + 2\nabla(S-\alpha).(\nabla\phi) \tag{2.10}$$

The twist layer of Figure 2 is formed when a nematic liquid crystal sample is sandwiched between two treated surfaces which induce strong homogeneous boundary conditions (i.e. the director is fixed parallel to the boundary). If one of the surfaces is twisted the torque exerted by the surface will induce a twist in the director field (Figure 5). When a field is applied to the cell it is possible to induce a concentration of the twisting into a small region of the cell. This high distortion region is a Helfrich wall [12]. It is a form of defect where the director is defined at *all* points in the cell (unlike in a line disclination

where the director is undefined along the line $r = 0$) but the orientation of the director is changed from one value to another across a very short distance. In this paper a twist cell with *no* applied field is considered but the liquid crystal scalar order parameters are allowed to vary. In this way Helfrich walls are obtained without a field where the minimization of the energy is possible due to melting around the wall.

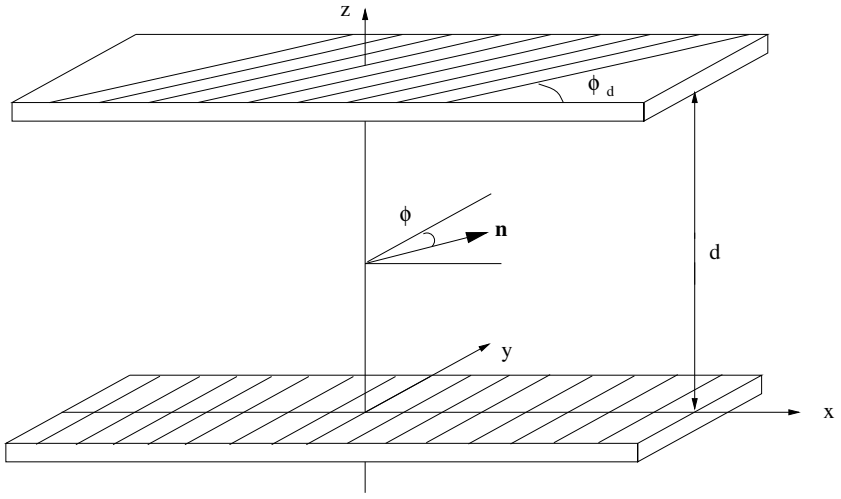

Figure 5: Schematic of a twisted nematic layer

For the twist layer shown in Figure 5 it will be assumed that all dependent variables depend only on the z coordinate and the free energy (2.7) becomes,

$$F_D = \frac{K}{2}\left(\frac{2}{3}S_z^2 + 2\alpha_z^2 + 2(S-\alpha)^2(\phi_z)^2 + \kappa_1\sigma_1(S) + \kappa_2\sigma_2(\alpha)\right) \tag{2.11}$$

where ϕ is the azimuthal or twist angle, that is the angle in the xy-plane from the director to the x axis. The other two dependent variables are the uniaxial scalar order parameter S and the degree of biaxiality α. The Euler-Lagrange equations are then,

$$0 = S_{zz} - 3(S-\alpha)(\phi_z)^2 - \frac{3\kappa_1}{4}\frac{\mathrm{d}\sigma_1}{\mathrm{d}S} \tag{2.12}$$

$$0 = \alpha_{zz} + (S-\alpha)(\phi_z)^2 - \frac{\kappa_2}{4}\frac{\mathrm{d}\sigma_2}{\mathrm{d}\alpha} \tag{2.13}$$

$$0 = \Big((S-\alpha)^2(\phi_z)\Big)_z \tag{2.14}$$

which with the potentials (2.5, 2.6) become,

$$
\begin{aligned}
0 &= S_{zz} - 3(S-\alpha)\phi_z^2 - \frac{3\kappa_1}{4}S(S-S_u)(S-S_b) && (2.15)\\
0 &= \alpha_{zz} + (S-\alpha)\phi_z^2 - \frac{\kappa_2\alpha}{4} && (2.16)\\
0 &= \Big((S-\alpha)^2\phi_z\Big)_z && (2.17)
\end{aligned}
$$

Without loss of generality $\phi = 0$ on $z = 0$ is assumed and the general form of the homogeneous boundary conditions of ϕ is,

$$
\begin{aligned}
\phi &= 0 \quad \text{on} \quad z = 0\\
\phi &= \phi_d \quad \text{on} \quad z = d
\end{aligned} \qquad (2.18)
$$

We use Dirichlet boundary conditions for S and α the general form of which are,

$$
\begin{aligned}
S &= S_0 \quad \text{on} \quad z = 0\\
S &= S_d \quad \text{on} \quad z = d\\
\alpha &= \alpha_0 \quad \text{on} \quad z = 0\\
\alpha &= \alpha_d \quad \text{on} \quad z = d
\end{aligned} \qquad (2.19)
$$

In Section 4 where the twist angle is $\phi_d = 0$, a solution is found for the general boundary conditions. However in Section 5 it is assumed that $S_0 = S_d$ and $\alpha_0 = \alpha_d$. It is also assumed that the boundaries prescribe a scalar order parameter $S_0 = S_d$ greater than the liquid crystal bulk scalar order parameter S_b and are uniaxial so that the boundary conditions are,

$$
\begin{aligned}
S_0 &= S_d > S_b && (2.20)\\
\alpha_0 &= \alpha_d = 0 && (2.21)
\end{aligned}
$$

The values $S_d = 0.8$ and $S_b = 0.7$ will therefore be taken throughout this paper. More general boundary conditions may be used in numerically solving

the governing equations but the above simplification gives the essential features of the defect structure within the layer. In the next section it is assumed that there is constant twist in the bulk of the layer and in Section 4 it is assumed that there is no twist. For these two cases analytic solutions to the governing equations are presented. In Section 5 the full equations are solved numerically using the continuation package AUTO.

3 Constant Twist

In this section, in order to understand our numerical results, we assume that there is constant twist throughout the cell. In this case $\phi_z = \lambda$. Then the equations (2.12, 2.13, 2.14) reduce to,

$$0 = S_{zz} - 3(S-\alpha)\lambda^2 - \frac{3\kappa_1}{4}\frac{\mathrm{d}\sigma_1}{\mathrm{d}S} \tag{3.22}$$

$$0 = \alpha_{zz} + (S-\alpha)\lambda^2 - \frac{\kappa_2}{4}\frac{\mathrm{d}\sigma_2}{\mathrm{d}\alpha} \tag{3.23}$$

$$0 = \left((S-\alpha)^2\lambda\right)_z \tag{3.24}$$

The third equation has solution,

$$S = \alpha \pm \sqrt{\frac{p}{\lambda}} \tag{3.25}$$

where p is constant. Substituting this into equation (3.22) and (3.23) gives,

$$0 = S_{zz} \mp 3\lambda^2\sqrt{\frac{p}{\lambda}} - \frac{3\kappa_1}{4}\frac{\mathrm{d}\sigma_1}{\mathrm{d}S} \tag{3.26}$$

$$0 = S_{zz} \pm \lambda^2\sqrt{\frac{p}{\lambda}} - \left.\frac{\kappa_2}{4}\frac{\mathrm{d}\sigma_2}{\mathrm{d}\alpha}\right|_{\alpha = S \mp \sqrt{\frac{p}{\lambda}}} \tag{3.27}$$

If S_{zz} is non-zero then for the two equations (3.26) and (3.27) to be consistent,

$$0 = \pm 4\lambda^2\sqrt{\frac{p}{\lambda}} + \frac{3\kappa_1}{4}\frac{\mathrm{d}\sigma_1}{\mathrm{d}S} - \left.\frac{\kappa_2}{4}\frac{\mathrm{d}\sigma_2}{\mathrm{d}\alpha}\right|_{\alpha = S \mp \sqrt{\frac{p}{\lambda}}} \tag{3.28}$$

In general, for a non-constant solution $S(z)$, this is not true for all z. The only solution is therefore S and α are constant. Substituting the potentials,

$$\sigma_1(S) = S^2\left(\frac{S^2}{4} - (S_u + S_b)\frac{S}{3} + \frac{S_u S_b}{2}\right) \tag{3.29}$$

$$\sigma_2(\alpha) = \frac{\alpha^2}{2} \tag{3.30}$$

into (3.26, 3.27) gives,

$$p = \lambda\left(\frac{S\kappa_2}{4\lambda^2 + \kappa_2}\right)^2 \tag{3.31}$$

and S must satisfy the cubic equation,

$$0 = S(S - S_u)(S - S_b) + \frac{4\lambda^2\kappa_2}{\kappa_1(4\lambda^2 + \kappa_2)}S \tag{3.32}$$

which, with $\lambda = \phi_d/d$ has the solutions,

$$S = 0 \tag{3.33}$$

$$\begin{aligned} S = {} & 0.5S_b + 0.5S_u + \Big((2\kappa_1 S_b^2\phi_d^2 + \kappa_1 S_b^2\kappa_2 d^2 - \\ & 4\kappa_1 S_u S_b\phi_d^2 - 2\kappa_1 S_u S_b\kappa_2 d^2 + 2\kappa_1 S_u^2\phi_d^2 + \\ & \kappa_1 S_u^2\kappa_2 d^2 - 8\kappa_2\phi_d^2)/2\kappa_1(4\phi_d^2 + \kappa_2 d^2)\Big)^{1/2} \end{aligned} \tag{3.34}$$

$$\begin{aligned} S = {} & 0.5S_b + 0.5S_u - \Big((2\kappa_1 S_b^2\phi_d^2 + \kappa_1 S_b^2\kappa_2 d^2 - \\ & 4\kappa_1 S_u S_b\phi_d^2 - 2\kappa_1 S_u S_b\kappa_2 d^2 + 2\kappa_1 S_u^2\phi_d^2 + \\ & \kappa_1 S_u^2\kappa_2 d^2 - 8\kappa_2\phi_d^2)/2\kappa_1(4\phi_d^2 + \kappa_2 d^2)\Big)^{1/2} \end{aligned} \tag{3.35}$$

Then α is calculated using (3.25) with (3.31) so that,

$$\alpha = \left(\frac{1}{1 + (\kappa_2 d^2)/4\phi_d^2}\right)S \tag{3.36}$$

The two solutions (3.34) and (3.35) are real when,

$$\frac{1}{\lambda} = \left(\frac{d}{\phi_d}\right)^2 > \frac{16}{\kappa_1(S_b - S_u)^2} - \frac{4}{\kappa_2} \tag{3.37}$$

If this condition is not met then the only solution is $S = 0$. It will be seen in later sections that there are certain regions in the ϕ_d-d parameter space where the bulk of the liquid crystal has melted so that $S = 0$, regions where the order parameter is close to S_b and some regions where it is possible to

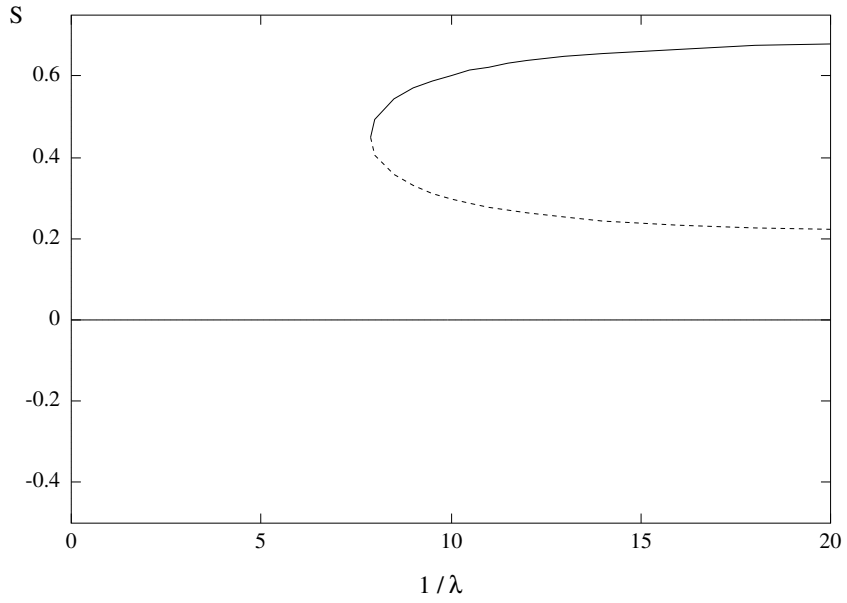

Figure 6: Solutions for constant S in a constant twist cell with parameter values $S_b = 0.7$, $S_u = 0.2$, $\kappa_1 = \kappa_2 = 1$.

obtain both forms of solutions. The above solutions for S (3.33, 3.34, 3.35) are shown in Figure 6.

When assessing the stability of these and any subsequent solutions we associate stable solutions with local minimisers of the free energy and unstable solutions with local maximisers of the free energy. In the above analysis we see that below $\lambda = 0.13$ there are three solutions, one melted ($S = 0$) and one liquid crystal ($S > 0.45$), both of which are stable and one unstable solution ($0 < S < 0.45$) (due to the two minima and one maximum of the potential function $\sigma_1(S)$). In all following diagrams stable solutions will be indicated by solid lines (and occasionally dotted lines when multiple solutions are plotted) and unstable solutions will be indicated by dashed lines.

4 No Twist

We now assume that $\phi_z = 0$ throughout the sample and take $\phi_0 = \phi_d = 0$. Using the potentials discussed in Section 2 the governing equations reduce to,

$$
\begin{aligned}
0 &= S_{zz} - \frac{3\kappa_1}{4} S^2 (S - S_u)(S - S_b) && (4.38)\\
0 &= \alpha_{zz} - \frac{\kappa_2}{4}\alpha && (4.39)
\end{aligned}
$$

with the boundary conditions,

$$
\begin{aligned}
S(0) &= S_0\\
S(d) &= S_d\\
\alpha(0) &= \alpha_0 && (4.40)\\
\alpha(d) &= \alpha_d
\end{aligned}
$$

The solution to the second equation (4.39) subject to the boundary conditions (4.40) is,

$$
\alpha = \alpha_d \frac{\sinh\left(\sqrt{\kappa_1} z/2\right)}{\sinh\left(\sqrt{\kappa_1} d/2\right)} - \alpha_0 \frac{\sinh\left(\sqrt{\kappa_1}(z-d)/2\right)}{\sinh\left(\sqrt{\kappa_1} d/2\right)} \qquad (4.41)
$$

The first equation can be solved by multiplying the equation by S_z and integrating to obtain,

$$
0 = (S_z)^2 - \frac{3\kappa_1}{4}\sigma_1(S) + D_1 \qquad (4.42)
$$

where $\sigma_1(S)$ is the potential discussed in Section 2 and D_1 is a constant. It may be assumed, without loss of generality, that $S_0 \geq S_d$. There are then three possibilities,

1. $S(z)$ attains its maximum in the layer
2. $S(z)$ attains its minimum in the layer
3. $S(z)$ attains its minimum at $z = d$

Then (4.42) can be evaluated at the max/min point to obtain D,

1. $D_1 = \frac{3\kappa_1}{4}\sigma_1(S_{max})$
2. $D_1 = \frac{3\kappa_1}{4}\sigma_1(S_{min})$

3. $D_1 = \frac{3\kappa_1}{4}\sigma_1(S_d) - ((S_z)_d)^2$

where S_{max}, S_{min} are the maximum/minimum values of S and $(S_z)_d$ is the value of S_z at $z = d$. In all three cases the value of D_1 ensures that equation (4.42) does not imply an imaginary value for S_z.

Thus (4.42) has the solution,

$$z = \int_z^{S_0} \frac{\mathrm{d}S}{\left(\frac{3\kappa_1}{4}\sigma_1(S) + D_1\right)^{1/2}} + D_2 \tag{4.43}$$

which leads to the implicit solution given in Byrd and Friedman [3],

$$S(z) = \cos^{-1}\left(\mathrm{cn}((z - D_2)/g, k)\right) \tag{4.44}$$

where,

$$g = 1/\left(AB\right)^{1/2} \tag{4.45}$$

$$k^2 = \frac{(A+B)^2 - (2(S_0 - S_u))^2}{4AB} \tag{4.46}$$

where $A^2 = (S_0 - \mathrm{Re}(c))^2 + (\mathrm{Im}(c))^2$, $B^2 = (2S_u - S_0 - \mathrm{Re}(c))^2 + (\mathrm{Im}(c))^2$ and c and $\bar{c}$ are the complex roots of the polynomial, $\frac{3\kappa_1}{4}\sigma_1(S) + D_1$.

The two constants of integration, D_1 and D_2 can then be found using the boundary conditions $S(0) = S_0$ and $S(d) = S_d$. The solutions for S and α for particular parameter values are shown in Figure 7.

5 Numerical Solutions

The full equations (2.15, 2.16 and 2.17) with the boundary conditions (2.18, 2.19) may be solved using the numerical package AUTO [6]. Using this package it is also possible to investigate how the solution changes when parameters in the governing equations and boundary conditions are altered.

Figure 9 shows the S, α and ϕ solutions when $\kappa_1 = 1$, $\kappa_2 = 1$, $d = 9$, $S_0 = S_d = 0.8$, $S_b = 0.7$, $S_u = 0.35$, $\alpha_0 = \alpha_d = 0$ and $\phi_d = 1.6$. This solution may be compared to Figure 8 which is the analytic solution for no twist with the same parameter values. For the twist cell biaxiality, α, is present throughout the region and the scalar order parameter, S, is lower than the bulk

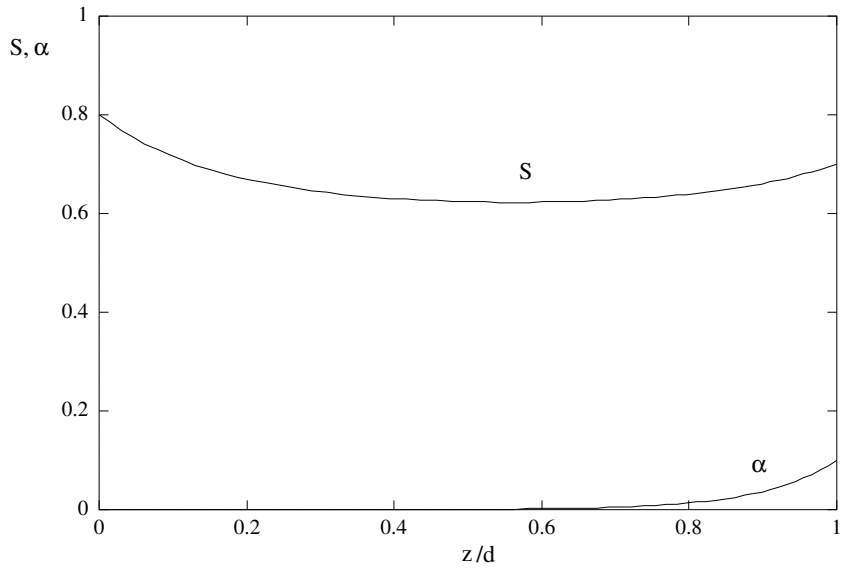

Figure 7: Solutions for S and α in a no twist cell with parameter values $S_0 = 0.8$, $S_d = 0.7$, $S_b = 0.6$, $S_u = 0.3$, $\alpha_0 = 0$, $\alpha_d = 0.1$, $\kappa_1 = \kappa_2 = 1$ and $d = 1$.

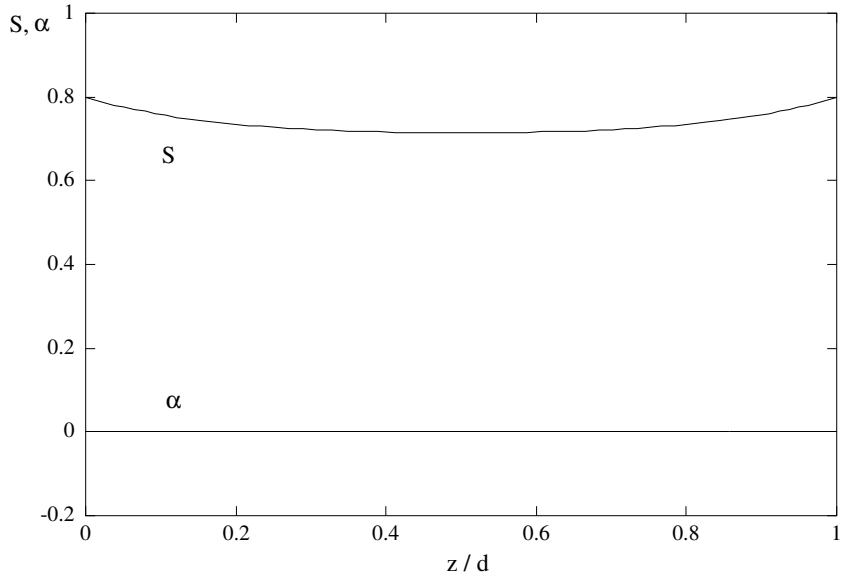

Figure 8: Solutions for S and α in a no twist cell with parameter values $S_0 = 0.8$, $S_d = 0.8$, $S_b = 0.7$, $S_u = 0.35$, $\alpha_0 = 0$, $\alpha_d = 0$, $\kappa_1 = \kappa_2 = 1$ and $d = 9$.

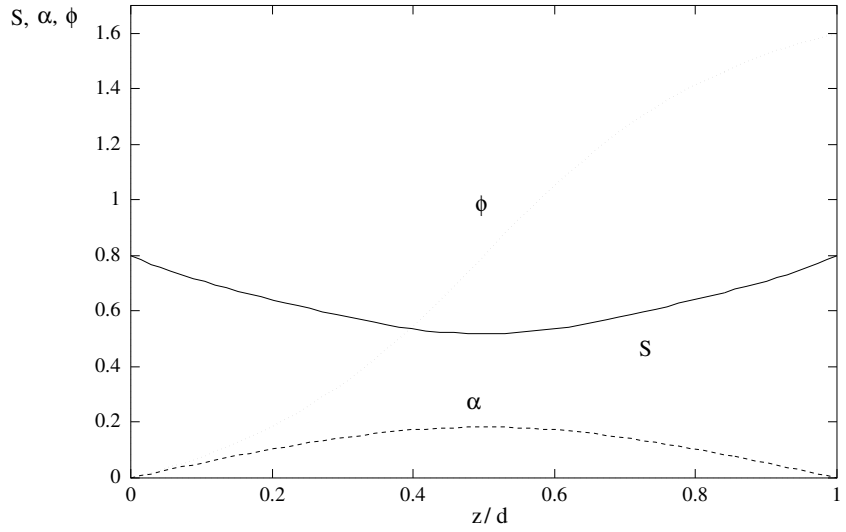

Figure 9: Twisted layer S, α and ϕ solutions for $\kappa_1 = 1$, $\kappa_2 = 1$, $d = 9$, $S_0 = S_d = 0.8$, $S_b = 0.7$, $S_u = 0.35$, $\alpha_0 = \alpha_d = 0$ and $\phi_d = 1.6$

scalar order parameter from the potential ($S_b = 0.7$) whereas in the no twist cell there is no biaxiality and the scalar order parameter never falls below $S_b = 0.7$.

The value of ϕ_z in Figure 9 shows that there is a larger amount of twist at the centre of the cell than at the boundaries and the scalar order parameter, S, reduces to compensate for the increased distortional energy. The other important point is that even though the biaxiality potential favours $\alpha = 0$ and the boundary conditions are $\alpha_0 = \alpha_d = 0$ there *is* biaxiality present in the cell. This is due to the second terms in (2.15) and (2.16). The relatively high twist at the centre leads to a high value of ϕ_z. The corresponding high energy is reduced by a decrease in $S - \alpha$ or alternatively a decrease in S and an increase in α.

It is now possible using AUTO to investigate the changes to this solution as the parameters vary. The main geometrical parameter is the gap width, d. Figure 10 shows the free energy $\mathcal{F}$ of the solution as AUTO follows the solution in Figure 9 whilst varying the gap width d with all other parameters fixed. There are two limit points, l_1 and l_2, in the solution branch at gap widths 8.4 and 29.7 between which there exists two stable solutions and one unstable solution. The units for the gap width cannot be found without knowing the

order of the potential coefficients κ_1 and κ_2. From an estimated value, for nematics, of κ_1 and κ_2 found in de Gennes and Prost [5] multiple solutions exist between gap widths of the order of 1-10 microns. The stable solutions are shown in Figures 11, 12 and 13 in this region for a gap width $d = 20$ corresponding to 6.32μm.

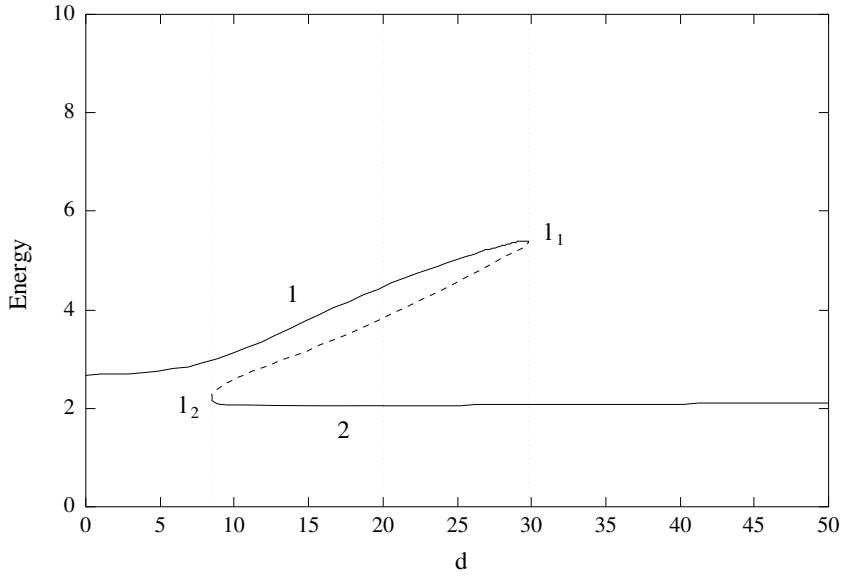

Figure 10: Fold in the energy as the gap width varies with the limit points l_1 and l_2 and the two stable solutions 1 and 2.

Solution 1 has almost uniform twist with a relatively high scalar order parameter S denoting a liquid crystalline state and a small amount of biaxiality. Solution 2 has a large twist gradient around the centre of the cell (near $z = d/2$), a corresponding region where the scalar order parameter S is low which indicates melting of the liquid crystal to an isotropic state and a concentration of biaxiality in the same region around $z = d/2$. This high energy distortion in solution 2 is compensated for by a decrease in the scalar order parameter S (Figure 11) and interestingly, although there is a concentration of the biaxiality around the centre of the cell, the maximum biaxiality α coefficient does not significantly increase (Figure 12).

The region where multiple solutions exist when other parameters are altered can now be investigated. The most interesting changes occur when the coefficient of the biaxial potential κ_2 is varied. As κ_2 is varied the package

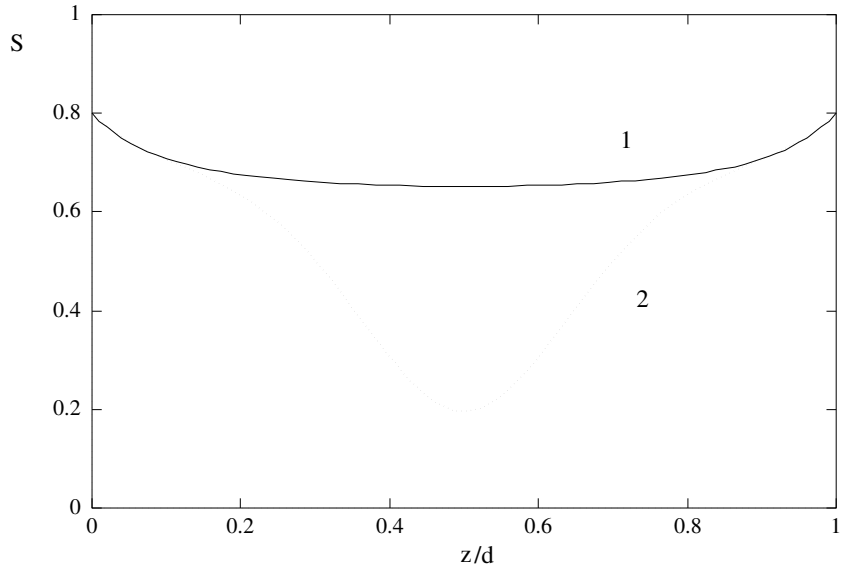

Figure 11: Multiple stable solutions of S in a twisted layer for d=20.

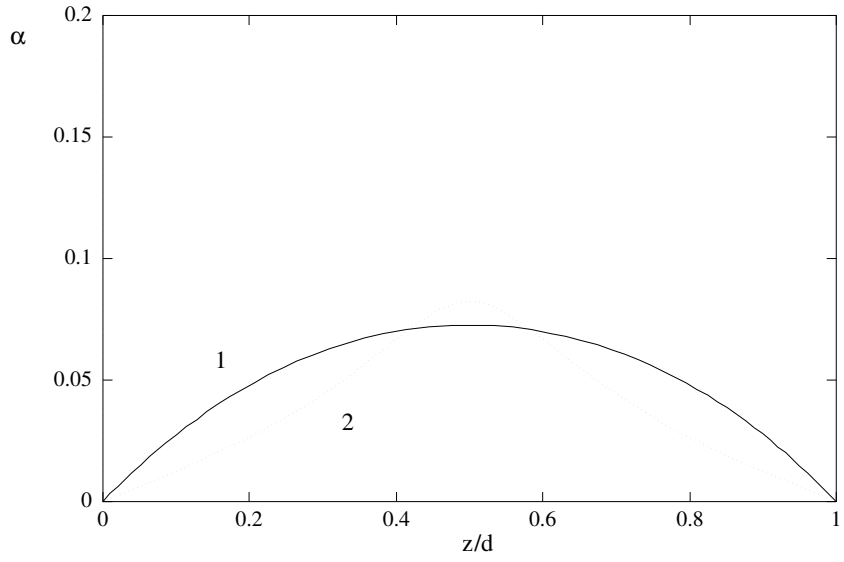

Figure 12: Multiple stable solutions of α in a twisted layer for d=20.

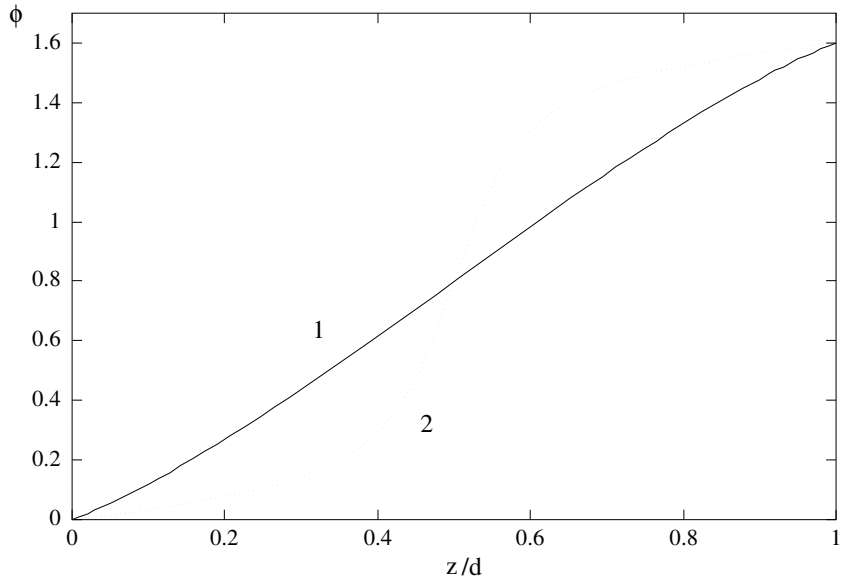

Figure 13: Multiple stable solutions of ϕ in a twisted layer for d=20.

AUTO finds the solutions to the equations and locates the two limit points l_1 and l_2 (in Figure 10). The region between these limit points is then where multiple solutions occur. Figure 14 shows this region up to a gap width of $d = 30$ where the numerical algorithm fails to converge to a solution. AUTO can find a solution along this branch for larger gap widths but it is difficult to *follow* the solution along this branch. By altering certain numerical parameters within AUTO and solving the equations for specific gap widths it is found that the locus of l_1 asymptotes to a straight line with gradient approximately equal to 1.

An increase in κ_2 makes biaxiality less favourable and when $\kappa_2 > 20$ biaxiality is energetically unfavourable and the liquid crystal is essentially uniaxial. Figure 14 shows that when there is biaxiality present in the layer ($\kappa_2 < 20$) multiple solutions only occur within a small range of gap widths. In fact when $\kappa_2 < 4.99$ there is only one biaxial solution for any gap width.

To investigate the multiplicity of solutions in this system κ_2 is fixed so that the liquid crystal is essentially uniaxial ($\kappa \gg 1$). We then take $\alpha = 0$ so that variations of S and ϕ need only be considered and the Euler-Lagrange equations are then,

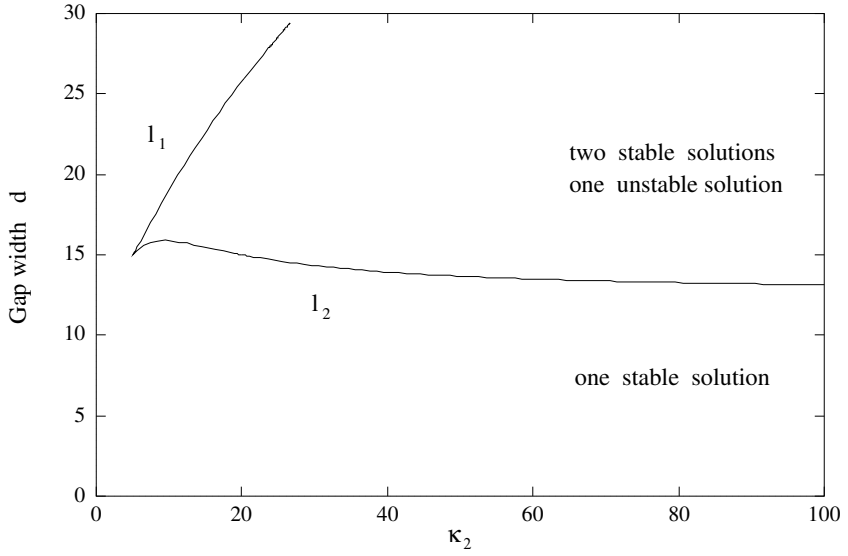

Figure 14: Locus of the limit points of Figure 10 forming a cusp in the κ_2, d parameter space

$$0 = S_{zz} - 3S\phi_z^2 - \frac{3\kappa_1}{4}S(S-S_u)(S-S_b) \tag{5.47}$$

$$0 = \left(S^2\phi_z\right)_z \tag{5.48}$$

S is nondimensionalised using $S^* = S/S_b$. Then the equations become,

$$0 = S^*_{zz} - 3S^*\phi_z^2 - \frac{3\kappa_1^*}{4}S^*(S^*-S_u^*)(S^*-1) \tag{5.49}$$

$$0 = \left((S^*)^2\phi_z\right)_z \tag{5.50}$$

with boundary conditions,

$$\phi(0) = 0 \tag{5.51}$$

$$\phi(d) = \phi_d > 0 \tag{5.52}$$

$$S^*(0) = S_0^* \tag{5.53}$$

$$S^*(d) = S_d^* \tag{5.54}$$

where $\kappa_1^* = \kappa_1 S_b^2$, $S_u^* = S_u/S_b$. The equation parameters are therefore κ_1^*, S_u^*, ϕ_d, d, S_0^* and S_d^*. Of these parameters only S_u^*, ϕ_d, d can be easily

changed within a liquid crystal cell in a physical situation, they correspond to temperature, the difference in twist between the two boundaries and gap width. In the present system which allows multiple stable solutions one solution of the equations exhibits a higher degree of melting than the other (Figures 11, 12, 13). The stability of these solutions is therefore expected to be affected by changes in S_u^* and will be investigated later in this section. The two parameters ϕ_d and d relate to the amount of twist in the layer and the distance over which the director must twist and it will be shown below that changes in these parameters critically affect the stability of the different possible solutions.

Variations of the gap width d and the amount of twist ϕ_d are initially considered. As before a solution is found for a specific set of parameters, $S_b = 0.7$, $\kappa_1 = 1$, $S_u^* = 0.5$, $\phi_d = 1.6$, $d = 9$, $S_0 = 0.8$. Figures 15 and 16 show the starting solutions for the above parameters.

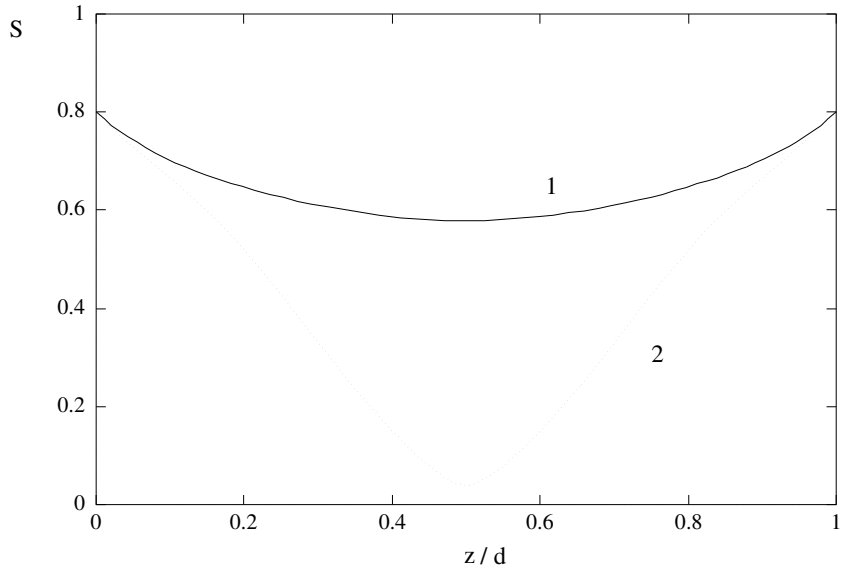

Figure 15: Uniaxial scalar order parameter stable solutions for a twist layer with parameters $S_b = 0.7$, $\kappa_1 = 1$, $S_u^* = 0.5$, $\phi_d = 1.6$, $d = 9$, $S_0 = 0.8$

If the solutions are followed as ϕ_d is continued through the range 0 to π the solution branches of the two solutions are linked by an unstable solution branch (Figure 17) and as in the biaxial case there are only three solutions in the range $\phi_d \in (1.36,\ 1.71)$ however there is no solution for angles past $\phi_d = 1.81$. After this point AUTO fails to converge on a solution and the L^2

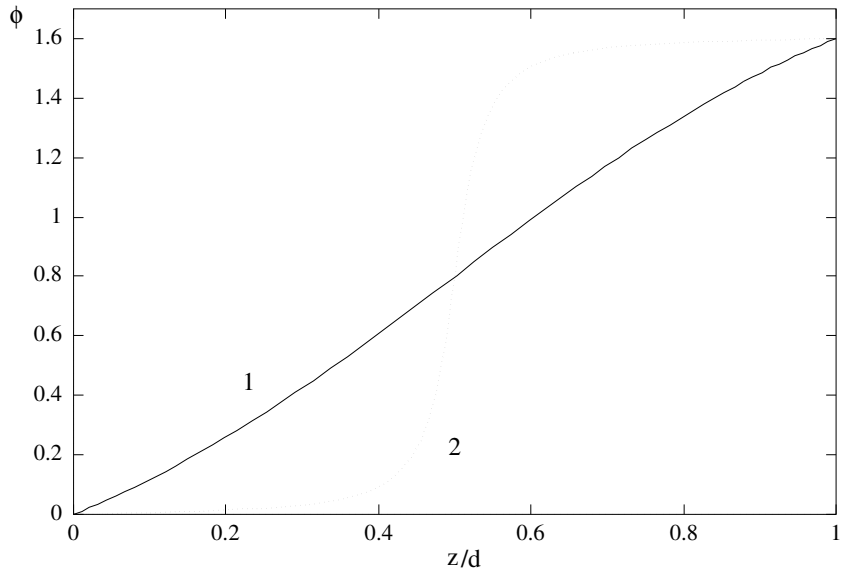

Figure 16: Uniaxial director angle stable solutions for a twist layer with parameters $S_b = 0.7$, $\kappa_1 = 1$, $S_u^* = 0.5$, $\phi_d = 1.6$, $d = 9$, $S_0 = 0.8$

norm which equals,

$$\|(S,\ \phi)\| = \int \sqrt{S^2 + (S_z)^2 + \phi^2 + (\phi_z)^2}\ \mathrm{d}z \tag{5.55}$$

tends to infinity (Figure 18). This failure to converge is due to the fact that the solution at this point in parameter space has extremely large values of ϕ_z near $z = d/2$. Figures 19 and 20 show the S and ϕ solutions for ϕ_d values before and after the fold.

There is a second possible configuration of the director for *any* point in parameter space due to the symmetry of the director. The directions $\mathbf{n}$ and $-\mathbf{n}$ are equivalent and therefore the director may twist in the opposite way from $\phi = 0$ on the lower boundary to $\phi = \phi_d + \pi$ on the upper boundary. There is therefore a second solution branch which is a reflection of the first in the line $\phi_d = \pi/2$ (Figure 21).

There are therefore two stable solutions when the twist parameter is in the regions $\phi_d \in (0,\ 1.36)$ or $\phi_d \in (1.78,\ \pi)$, there are three stable solutions and one unstable solution when $\phi_d \in (1.36,\ 1.43)$ or $\phi_d \in (1.71,\ 1.78)$ and there are four stable and two unstable solutions when $\phi_d \in (1.43,\ 1.71)$.

These regions, in which different numbers of solutions exist, can be investigated when another parameter is varied. Using AUTO the boundaries of

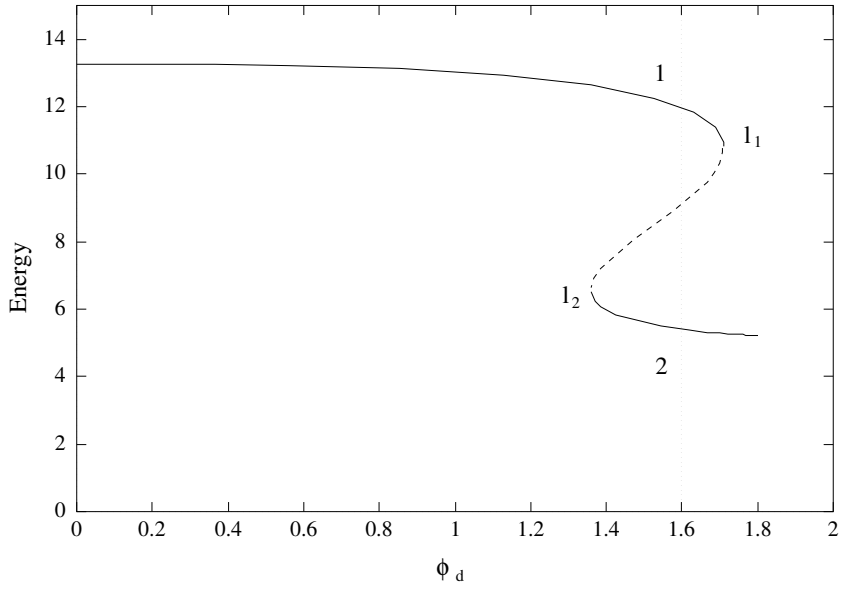

Figure 17: Fold in the Energy versus ϕ_d diagram for d=9.

the regions, which in this case are the limit point values of ϕ_d of the folds in Figure 20, may be followed as the gap width d is varied. Figure 22 shows the loci of the limit points values in the d, ϕ_d parameter space. For a cell with a gap width less than 6.49 there is only one possible solution. Between $d = 6.49$ and $d = 8.50$ the two cusps do not overlap so that there is a region around $\phi_d = \pi/2$ where there is one solution and within the cusp region there are two stable and one unstable solutions. After $d = 8.5$ the cusps overlap and there is a region around $\phi_d = \pi/2$ where there are four stable solutions and two unstable solutions possible at one point in parameter space.

As discussed before the parameter S_u has been set to be $S_b/2$ ($S_u^* = 0.5$) and hence the temperature is equal to the clearing point temperature T_c. At this point the two minima of the potential function are *both* global minimizers of the energy functional and hence the system can support multiple solutions. If the parameter S_u^* is changed so that the temperature is increased ($S_u^* \to 1$) or decreased ($S_u^* \to 0$) the system would be expected to prefer the high twist gradient, high melting solution or the uniform twist, low melting solution respectively. Figure 23 shows the development of one of the cusps from Figure 22 as S_u^* ($= S_u/S_b$) varies from 0 to 1.

Between the two cusps for $S_u^* = 0.5$ and $S_u^* = 0.55$ the asymptotic behaviour

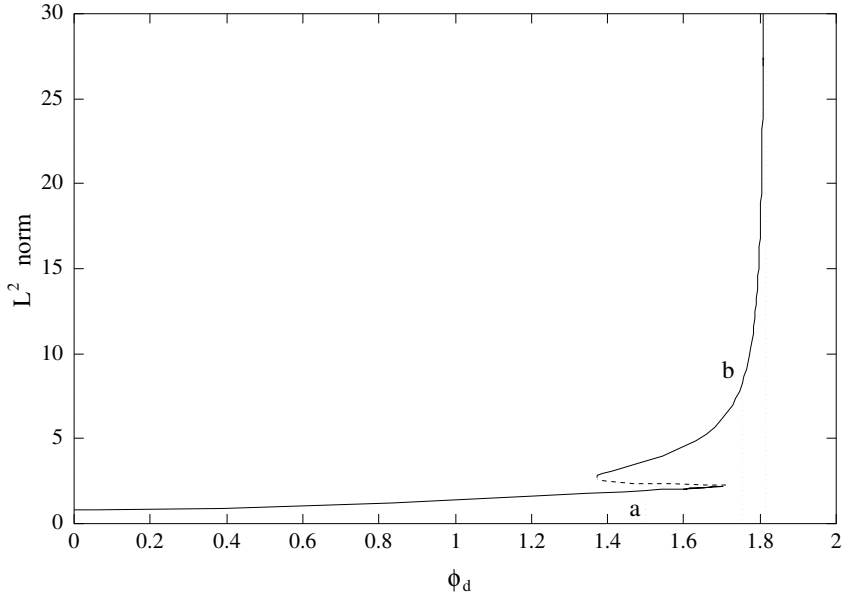

Figure 18: Fold and singularity in the L^2 norm versus ϕ_d diagram.

of the cusp changes. Less than a critical value of S_u^* the lower branch of the cusp asymptotes to a fixed twist parameter. More than the critical parameter and the branch asymptotes to a fixed gap width. If S_u^* is high enough then for any value of the twist parameter there is a solution that involves melting and is the lowest energy solution. If S_u^* is lower than the critical value and if the twist parameter is low enough then the only solution is that with uniform twist and no melting.

6 Discussion

We have considered wall defects within twisted nematic layers. Analytical solutions are found for two cases. When only the bulk of the liquid crystal layer is considered a solution is found for *constant* twist and for the whole system (including the boundary effects) with *no* twist present in the layer the governing equations uncouple and an analytic solution can be found. The full equations with twist present have been solved using the numerical continuation package AUTO. Once a solution is obtained we investigated the effect of various changes to the parameters. In certain regions in parameter space there exist more than one solution to the equations.

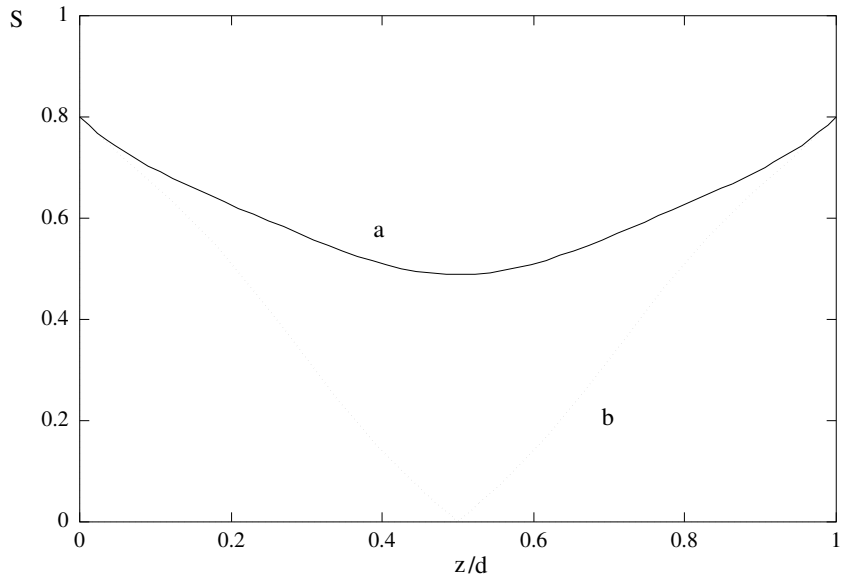

Figure 19: S solutions before the fold (a) and after (b) the fold near the L^2 norm singularity.

The symmetry of the system (reflection in the line $\phi_d = \pi/2$) leads to regions where 4 stable and two unstable solutions exist, regions where two stable and one unstable solution exist and regions where only one stable solution exists. Typically the stable solutions are of two kinds. The first solution involves a uniform twist between the two boundaries and a small decrease in the scalar order parameter compared to the no-twist case. The second solution is a wall defect where the twisting necessary in the layer is concentrated around the centre at $z = d/2$ and the scalar order parameter decreases to values close to zero. The liquid crystal has therefore melted to an isotropic liquid in this region.

Figure 22 shows that for a greater amount of twist in the layer (ϕ_d larger) the wall defect solution will become the only stable solution and for less twist in the layer (ϕ_d smaller) the uniform twist solution will become the only stable solution and in the region in the middle both solutions are stable and the system exhibits hysteresis. Changes in the gap width, d, then determine the size of this region. As the gap width increases the director stress from the twist distortion decreases and the non-melting/uniform twist solution is stable over a larger range of twist angles ϕ_d.

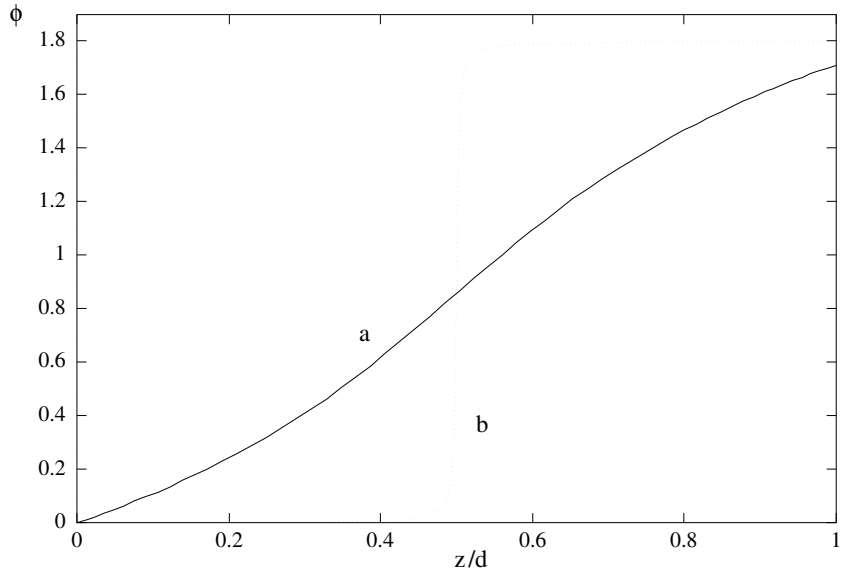

Figure 20: ϕ solutions before the fold (a) and after (b) the fold near the L^2 norm singularity

Figure 23 shows that as the temperature increases (S_u increases) the asymptotic nature of the cusps in Figure 22 change. For values of S_u greater than a critical value the wall defect solution is stable (for d greater than some critical value) for any twist angle ϕ_d, even when there is no twist present. The critical dependence on S_u of the form of the cusp may be thought of as a phase transition. The system prefers the liquid crystal state below the critical S_u and the isotropic state above the critical value. This nematic-isotropic phase transition occurs between $S_u^* \in (0.5,\ 0.55)$ so that the nematic state is still stable above the classical critical temperature T_c but before the temperature T^+ when the nematic state loses local stability and is similar to the phase transition seen in a previous paper by the authors [13].

It is important to realise that in certain parameter regions there may form a twist wall which will greatly affect the performance of the twist cell. The display would essentially be useless as there would be a layer of isotropic liquid within the cell and the incident light would not be guided by the director orientation to emerge through the second polarizer (see Figure 2). These regions in parameter space are present at all temperatures although for low temperatures multiple solutions are present only for cells containing large amounts

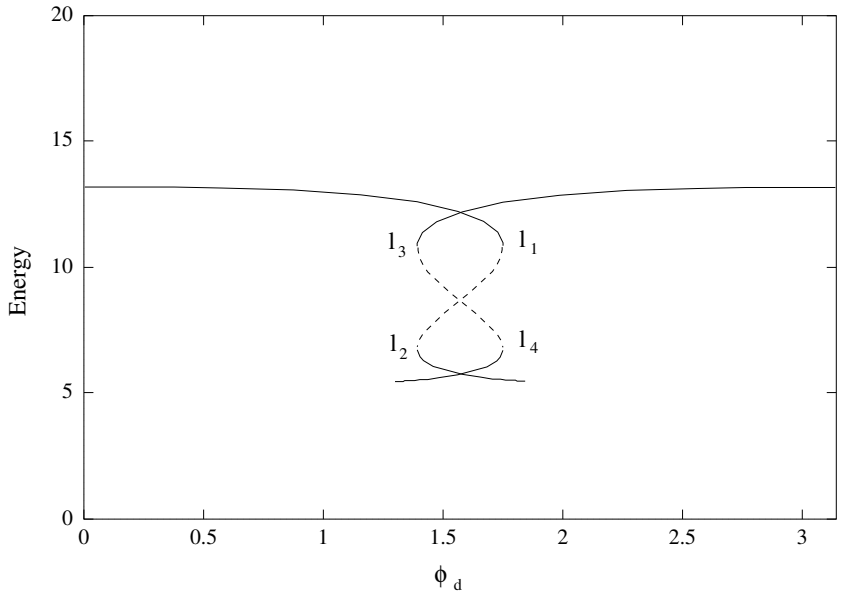

Figure 21: The effect of symmetry on the fold diagram is a reflection in the line $\phi_d = \pi/2$.

of twist. In most common TNLCD applications these regions are avoided but for the examples listed in the Introduction the region of low order may be crucial to its device usefulness. The estimated values of the parameter regions where multiple solutions exist, which were calculated in Section 5, will give a guideline as to how much twist is possible in these examples but for a more detailed analysis each of the systems should be treated separately.

It is hoped that future work will investigate the effect of an aligning electric field which has been shown to concentrate the twist deformation into small regions and induce cholesteric unwinding [5]. It is therefore expected that the presence of this field will encourage the formation of these regions of low orientational order.

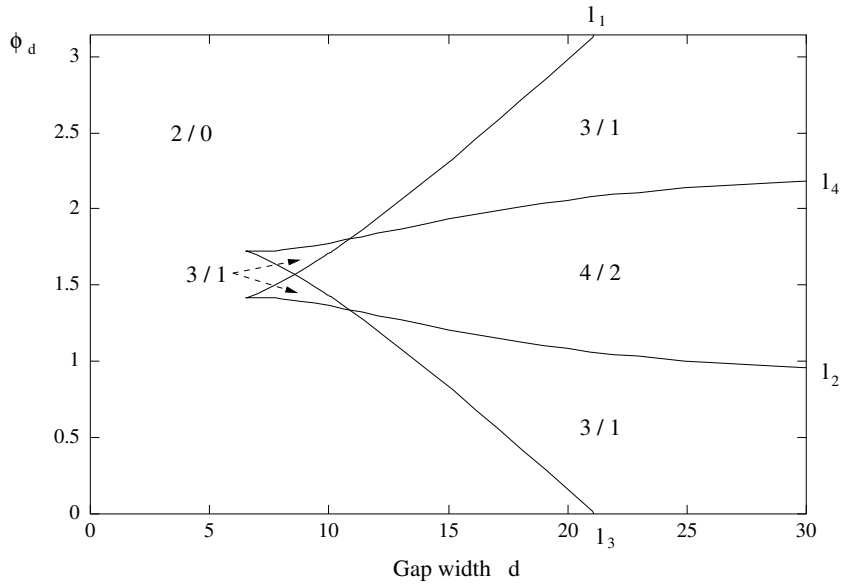

Figure 22: Locus of the *four* limit points (l_1, l_2, l_3 and l_4) in Figure 21 in the ϕ_d, d parameter space. In the regions i/j there exist i stable solutions and j unstable solutions.

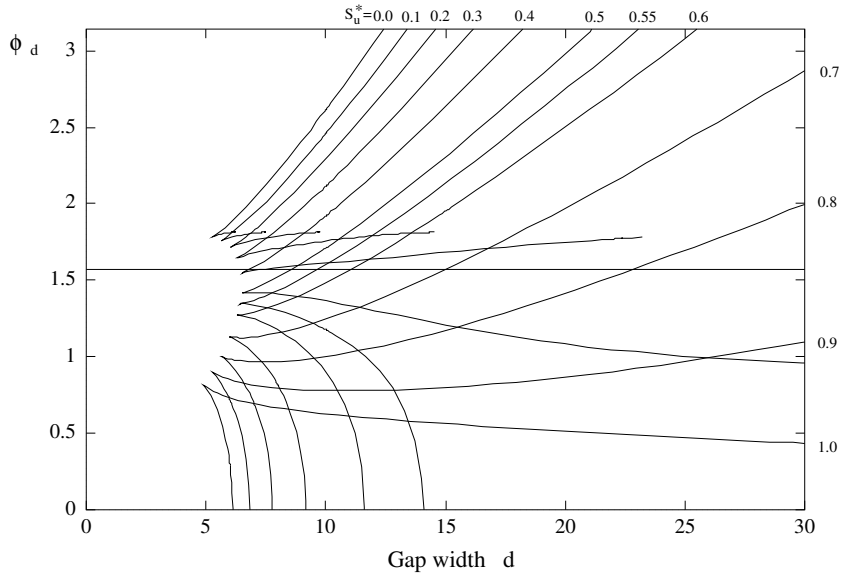

Figure 23: The change in one of the cusps (Figure 22) as S_u^* (or equivalently) temperature varies.

References

[1] D. W. Berreman and W. R. Heffner. New bistable liquid-crystal twist cell. *J. Appl. Phys.*, 52(4):3032–3039, 1981.

[2] P. Biscari and E. G. Virga. Biaxial nematics between two cylinders. *to appear in Intl. J. Nonlin. Mech.*, 1996.

[3] P. F. Byrd and M. D. Friedman. *Handbook of Elliptic Integrals for Engineers and Physicists.* Springer-Verlag, 1954.

[4] P. G. de Gennes. Phenomenology of short-range-order effects in the isotropic phase of nematic liquid crystals. *Phys. Lett. A*, 30:454, 1969.

[5] P. G. de Gennes and J. Prost. *The Physics of Liquid Crystals.* Oxford University Press (Clarendon Press), 2nd edition, 1993.

[6] E. J. Doedel. AUTO: A program for the automatic bifurcation analysis of autonomous systems. *Congressus Numeranti*, 30:265, 1981.

[7] M. Doi. Molecular dynamics and rheological properties of concentrated solutions of rod like polymers in isotropic and liquid crystalline phases. *J. Polymer Sci.*, 19:229, 1981.

[8] J. L. Ericksen. Liquid crystals with variable degree of orientation. *Arch. Rational Mech. Anal.*, 113:97, 1991.

[9] C. Fan. Disclination lines in liquid crystals. *Phys. Lett. A*, 34:335, 1971.

[10] F. C. Frank. On the theory of liquid crystals. *Discuss. Faraday Soc.*, 25:19, 1958.

[11] E. C. Gartland Jnr., P. Palffy-Muhoray, and R. S. Varga. Numerical minimization of the landau-de Gennes free energy: Defects in cylindrical capillaries. *Mol. Cryst. Liq. Cryst.*, 199:429, 1991.

[12] W. Helfrich. *Phys. Rev. Lett*, 21:1518, 1968.

[13] N. J. Mottram and S. J. Hogan. Disclination core structure and induced phase change in nematic liquid crystals. *Phil. Trans. Roy. Soc (to appear)*, 1997.

[14] M. Oh-e and K. Kondo. The in-plane switching of homogeneously aligned nematic liquid crystals. *Liquid Crystals*, 22(4):379–390, 1997.

[15] C. W. Oseen. The theory of liquid crystals. *Trans. Faraday Soc.*, 29:883, 1933.

[16] D. Roccato and E. G. Virga. On plane defects in nematic liquid-crystals with variable degree of orientation. *Continuum Mechanics and Thermodynamics*, 4(2):121, 1992.

[17] N. Schophol and T. J. Sluckin. Defect core structure in nematic liquid crystals. *Phys. Rev. Lett.*, 59(22):2582, 1987.

[18] E. G. Virga. *Variational Theories for Liquid Crystals*. Chapman & Hall, 1991.